Artificial neural network to predict traction performance of autonomous ground vehicle on a sloped soil bin and uncertainty analysis

Article *in* Computers and Electronics in Agriculture · March 2022

DOI: 10.1016/j.compag.2022.106867

CITATIONS
7

READS
49

3 authors:

Chetan Badgujar
Kansas State University
16 PUBLICATIONS **32** CITATIONS
SEE PROFILE

Daniel Flippo
Kansas State University
30 PUBLICATIONS **102** CITATIONS
SEE PROFILE

Stephen Welch
Kansas State University
129 PUBLICATIONS **3,719** CITATIONS
SEE PROFILE

Computers and Electronics in Agriculture 196 (2022) 106867

Contents lists available at ScienceDirect

Computers and Electronics in Agriculture

journal homepage: www.elsevier.com/locate/compag

Artificial neural network to predict traction performance of autonomous ground vehicle on a sloped soil bin and uncertainty analysis

Chetan Badgujar [a,*], Daniel Flippo [a], Stephen Welch [b]

[a] Biological & Agricultural Engineering, Kansas State University, Manhattan, KS 66502, United States
[b] Department of Agronomy, Kansas State University, Manhattan, KS 66502, United States

ARTICLE INFO

Keywords:
Multi-AGV
Tractive efficiency
Power number
Drawbar pull test
Travel reduction
K-fold cross validation

ABSTRACT

A fleet of autonomous ground vehicles (AGV) is envisioned to expand farming to arable land suitable for production except for being too steep for conventional equipment. The success of proposed multi-AGV system largely depends on the traction performance of the individual AGVs on unevenly sloped terrain and optimization of the AGVs control variables. Therefore, the drawbar pull performance of a prototype AGV was evaluated in a soil bin at varying slopes, speeds, and drawbar pull (DP). The AGV's traction performance was expressed in three metrics: tractive efficiency (TE), travel reduction ratio (TRR), and power number (PN). Optimizing the control variables is intricate and ill-defined, which requires an accurate model to predict the performance of the proposed multi-AGV system. Hence, this study aims to design an artificial neural network (ANN) to estimate the traction behavior of the AGV on a sloped testbed as a function of AGV's speed, applied DP, and slope. A multilayer perceptron feed-forward ANN architecture with a single hidden layer trained with a back-propagation algorithm was adopted. A series of ANN models with increasing complexity and different hidden layer activation functions were developed for each response variable, i.e., ANN-TE, ANN-TRR, and ANN-PN. A re-sampling-based method, K-fold cross-validation, was employed to estimate the model generalization error. The model success was evaluated via Mean Squared Error (MSE) and the Coefficient of Determination (R^2) against a test set. The final predictive model was trained on the entire data set, and the observed R^2 was 0.933, 0.882 and 0.858, respectively, for ANN-TE, ANN-TRR, and ANN-PN. Subsequently, a Monte-Carlo Simulation based uncertainty analysis was carried out to demonstrate the model strength and the degree of uncertainty by constructing a 95% prediction interval. This study shows ANN as a promising, robust, and reliable method to predict traction performance in agricultural tillage-traction studies and developed models can empower the multi-AGV system on steep-uneven slope terrain.

1. Introduction

Cropland expansion remains one of the leading factors in global agricultural production growth to meet the rising demands of food, fiber, and fuel of an escalating population (Foley et al., 2011; Gregory and George, 2011; Zabel et al., 2019). However, hills, uneven terrain, and excessive steepness of grassland (> 6°) preclude farming with conventional agricultural machines (Foley et al., 2011). On sloping terrain, tractor rollovers are more frequent and one of the leading causes of farmer injury and/or death during farm operations (Myers et al., 2009; Myers and Hendricks, 2010). This impediment could be potentially and sustainably addressed with a fleet of small autonomous ground vehicles (AGV). Multi-AGV systems are rapidly gaining interest for smart farming and are prime candidates for future outdoor agriculture (Bechar and Vigneault, 2016; Gonzalez-De-Santos et al., 2020). AGVs can accomplish work equivalent to a large conventional machine but with reduced soil compaction, better accuracy and can be programmed to work at peak efficiency without human intervention (García-Pérez et al., 2008; Emmi et al., 2013; Emmi et al., 2014; Conesa-Muñoz et al., 2015; Li et al., 2015; Zhang et al., 2016). There is abundant evidence suggesting robots/AGVs can perform various agricultural operations, including seeding and transplanting (Hu et al., 2014; Haibo et al., 2015; Amrita et al., 2015), plant protection and weed control (Pérez-Ruíz et al., 2014; Choi et al., 2015), fruit-vegetable harvesting (De-An et al., 2011; Li et al., 2013; Mehta and Burks, 2014); with robust field localisation and mapping (Se et al., 2005; Jagbrant et al., 2015;

* Corresponding author.
E-mail address: chetan19@ksu.edu (C. Badgujar).

https://doi.org/10.1016/j.compag.2022.106867
Received 24 September 2021; Received in revised form 7 March 2022; Accepted 9 March 2022

Bayar et al., 2015).

The success of the proposed multi-AGV system largely depends on the traction performance of the individual AGVs on unevenly sloped terrain. Traction performance is defined by the net traction ratio and the tractive efficiency (Burt et al., 1980; Ekinci et al., 2015), which quantifies the amount of tractive effort generated for the agricultural task, power consumed, and nature of the agricultural operation (i.e., tillage types and inputs carrying capacity) the AGV could perform. Major factors affecting ground vehicle performance on sloping terrain are terrain tilt, operating direction (uphill, downhill, sideways), lateral slippage, applied drawbar pull, and vehicle speed (Zhu et al., 2005). Therefore, to understand sloped terrain AGV performance, controlled laboratory experiments must be carried out to develop models explaining the influence of the AGV's operational variables on these parameters. The resulting models can describe vehicle behavior, help to improve the vehicle design, optimize operational parameters, and minimize energy consumption. Furthermore, a performance model from limited laboratory experiments can be extended to a dynamic terrain environment for decision support system, path planning, route optimization, power optimization, and so on.

In the last few decades, a variety of modeling techniques including analytical, empirical, and semi-empirical, have been implemented to predict or measure the traction performance of both wheeled and tracked vehicles either on controlled soil bin conditions or unprepared fields (Freitag, 1966; Wismer and Luth, 1974; Yong and Fattah, 1976; Hayes and Ligon, 1981; Wong, 1986; Colin et al., 1987; Dwyer, 1987; Upadhyaya et al., 1989; Wang and Domier, 1989; Nakashima and Oida, 2004; Tiwari et al., 2010). These models helped to understand and establish vehicle traction performance (primarily tractor) to improve and optimize its operational parameters (Tiwari et al., 2010). In analytical methods, traction parameters are determined from soil-tire/track contact surface geometry and stress distribution (normal and shear). Nevertheless, the complex nature of soil-tire interactions, varying soil parameters, and inadequate information of boundary conditions are major challenges for its adoption (Tiwari et al., 2010; Sunusi et al., 2020). Empirical traction models are obtained from large amounts of experimental data, and often yield constants and coefficients pertaining to specific experimental conditions. This restricts their applicability in a dynamic agricultural environment as well as for different vehicle type/configurations (Tiwari et al., 2010; Wong, 2010). Semi-empirical models are easy to use, derived from both experimental data and fundamental analysis of soil-tire interaction. However, assumption-dependent model development processes limit their accuracy in different terrain and vehicle types.

The limitation of existing modeling techniques, demand for models with better prediction capabilities and advancements in data-driven computer science have inspired researchers to develop traction models based on machine learning approaches, such as artificial neural networks (ANN). ANN is a robust modeling method that draws on loose analogies to natural neural tissue combined with an automated model selection process. In recent years, ANN has emerged as promising tool to model and analyze very complex problems in biological and agricultural domains (Huang et al., 2010). ANN has been widely used to predict the traction performance of tractors and tillage implements as affected by various machine and soil parameters (Tohmaz and Hassan, 1995; Zhu et al., 2005; Taghavifar and Mardani, 2014; Taghavifar and Mardani, 2014; Taghavifar et al., 2015; Ekinci et al., 2015; Almaliki et al., 2016; Shafaei et al., 2018; Pentos et al., 2020).

The predictive capability of several ANN configurations was assessed by Almaliki et al. (2016) for tractor performance, in terms of tractive efficiency, drawbar power, rolling resistance, and fuel consumption. Their results confirmed ANN ability to learn the relationships among input variables and tractor performance parameters. Ekinci et al. (2015) designed seven different ANN models with a single hidden layer to predict the tractive performance (tractive efficiency) of radial tires fitted on off-road vehicles. Given inputs of lug height, axle load, inflation pressure, drawbar pull, and trained with the Levenberg–Marquardt algorithm, the resulting ANN successfully predicted tractive efficiency. While, as exemplified by the citations just above, ANNs have frequently been used to model the performance of human-operated tractors, to the best of our knowledge, this has not been done for AGVs. Neither, apparently, has terrain slope been used as a predictor variable and its influence on AGV's traction performance is unknown to date.

ANN model development is stochastic in nature, and an identical ANN trained on the same data produced different results on each run owing to random data splitting methods and random ANN parameter initialization. Therefore, it is necessary to quantify the prediction uncertainty of the final model, especially given that it will be utilized to optimize control variables and decision making. Uncertainty analysis (UA) assesses the model output error and quantifies the output variability based on input variability. Monte-Carlo Simulation (MCS) is a well-established technique to quantify uncertainty of ANN model prediction. It computes the model error emerging from data uncertainty (inherent noise) and model uncertainty. The MCS was first proposed by Marcé et al. (2004) for ANN and since then has been implemented in several other studies, mostly in environment and climate (Noori et al., 2010; Dehghani et al., 2014; Antanasijevic et al., 2014; Lee et al., 2020). However, very little if any information is available on ANN uncertainty analysis in agricultural tillage and traction domain.

Therefore, the objective of this study is to develop an ANN model to predict AGV traction performance in a sloped soil bin as a function of slope, speed and drawbar pull. Moreover, to investigate the output uncertainty of the developed ANN model, an MCS-based uncertainty analysis was carried out. The resulting traction prediction model would improve vehicle performance by optimizing its operational variables and establish the boundary conditions on sloped terrain. Moreover it would assist in vehicle design, safety, and optimizing the energy and mobility aspects on highly sloped and uneven terrain.

2. Materials and Methods

To develop the AGV's traction model, a large amount of data is a prerequisite. A standard drawbar pull (DP) test characterizes off-road vehicle performance (Creager et al., 2017) and measures a vehicle's total tractive ability (Wong, 2010b). Thus, a DP performance of the AGV was carried out in a soil bin on a testbed slope ranging from 0-20° for both uphill and downhill runs. The soil bin was 5.0 m long, 2.5 m wide and 0.2 m deep, equipped with hydraulic lift attachments to vary the slope. The DP test was conducted at Department of Biological and Agricultural Engineering, Kansas State University, Manhattan, KS, USA and the generated data was used to develop the AGV's traction model.

2.1. Experiment setup

2.1.1. AGV and soil bin

A continuous track-type AGV prototype (Fig. 1) was used in the study and its technical details are tabulated in Table 1. The prototype is equipped with a micro-controller (myRio, National Instruments, Austin, TX, USA), proprioceptive sensors (amperage-voltage and track encoders), and a rechargeable Lithium Polymer (Li-Po) battery with a capacity of 52 Ah and 22.2 V. The AGV is teleoperated, connected wirelessly to a tablet computer (iPad, Apple Inc, Cupertino, CA), and controlled by the operator.

Soil condition influences the DP performance (Domier and Willans, 1978; Hayes and Ligon, 1981). Therefore, uniform soil conditions were maintained and assumed throughout the soil bin (hereafter referred to as testbed) for all the slope testing. Testbed soil preparation included soil loosening, pulverization and leveling (Creager et al., 2017). However, repeated passes of AGVs compacted the soil, cumulatively increasing the soil bulk density. Thus, a straight leaf rake was used for soil loosening and leveling. Before conducting the DP test, the testbed condition was measured as follows. The cone index (CI) measure of soil strength was

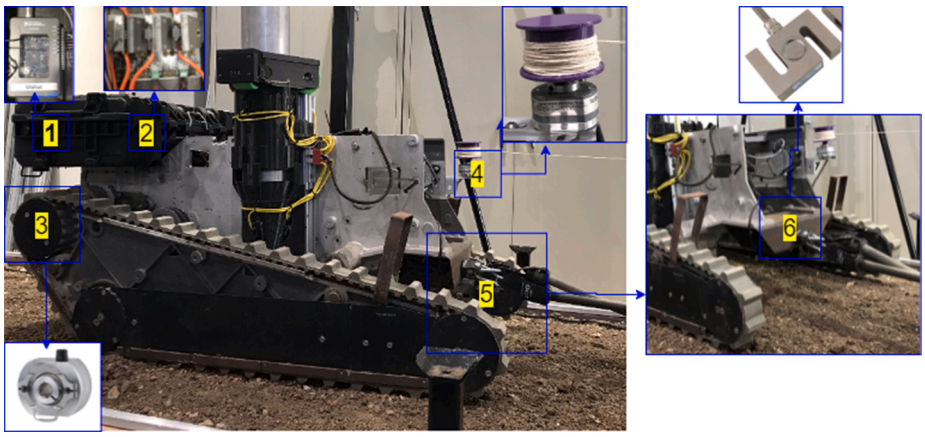

Fig. 1. DP test experimental setup, (1) micro-controller (myRio), (2) Amperage-voltage sensor, (3) track encoder, (4) ground truth encoder, (5) resistance rubber band and (6) load cell.

Table 1
Technical details of the AGV and fitted track.

AGV		Track	
Mass, kg	102	Track style	Continuous
Length, mm	1160	Thickness, mm	5
Width, mm	640	Belt width, mm	50
Height, mm	550	Belt contact length, mm	2410
Gauge, mm	500	Lug height, mm	12
Longitudinal CG location from front axis, mm	400	Sprocket to idler center distance, mm	910
Longitudinal CG location from rear axis, mm	700	Diameter of sprockets and idler, mm	126
Vertical CG location, mm	200	Pitch, mm	55
Hitch height, mm	200		

recorded according to ASABE standards (Standards, 2019) up to a depth of 150 mm at eight randomly selected locations along the testbed. The CI gradient (kPa/mm) was also computed from available data, which describes the density and consistency of the soil (Creager et al., 2017). Six samples of soil bulk density and water content were taken randomly on the testbed; cylinder method and standard oven-dry methods (IS 2720–2, 1993) were used, respectively. The testbed characteristics such as soil bulk density (g cm^{-3}), water content (%), cone index (kPa), and CI gradient (kPa mm^{-1}), were evaluated and average values are reported in Table 2. A multiple comparison procedure (Least Significant Difference, LSD) was performed to detect any significant departures from soil uniformity on the testbed.

2.1.2. Instrumentation setup

The prototype AGV was properly instrumented to precisely measure each track's velocity, power consumption and applied DP. The AGV's track slip is derived from actual track velocity (v) and reference velocity (v_{ref}). To measure the actual velocity (v), a ground truth encoder was mounted on AGV's chassis and consists of a 3D printed spool with a cotton thread, mounted on the encoder shaft. As the AGV moves on the testbed thread gets unwrapped from the spool, which rotates the encoder shaft (Fig. 1). Reference velocity (v_{ref}) is obtained from the fitted track encoder data and measured track rolling radius. A resistance rubber band was used to apply variable DP (F_{DP}) to the AGV (see next section). A pre-calibrated S-type load cell installed between AGV's hitch point and the rubber band measured the applied DP. The AGV's power consumption (P) was measured with amperage-voltage sensors. Data from the load cell, each track encoder, ground-truth encoder, and amperage-voltage sensors were recorded by a micro-controller (myRio), at a frequency of 10 Hz and stored in a 64 GB USB thumb-drive. A digital protractor was used to set the desired testbed inclination. The AGV weight (w) was recorded with standard weight scale. The technical specifications of the sensors used in the study are listed in Table 3.

Table 2
Mean and deviation of testbed soil characteristic.

Testbed slope (°)	Cone Index (kPa)	CI gradient (kPa mm^{-1})	Water content (% db)	Bulk density (g cm^{-3})
0 (S_0)	493.3 ± 92.3	2.5 ± 0.5	17.2 ± 4.0	1.5 ± 0.1
10 (S_{10})	464.4 ± 97.6	2.4 ± 0.5	18.8 ± 5.7	1.4 ± 0.1
18 (S_{18})	461.5 ± 59.8	2.4 ± 0.3	18.5 ± 1.8	1.6 ± 0.04
p-value	0.73	0.73	0.77	0.02

2.2. Laboratory experiments

The soil bin slope was fixed to the desired slope inclination angle and uniform soil properties were maintained during the DP test. A ramped-DP test technique was employed, which tests an entire range of DP from zero (self-propelled condition) to the maximum DP (immobilized condition) in a single run (Woodward, 2011; Creager et al., 2017). During the DP test, the AGV was operated on the desired duty cycle via an iPad device. As the AGV moves on the testbed, the resistance band ramps up

Table 3
Technical specification of the sensors used in the study.

Sensor	Model and Manufacture	Specification	Accuracy
Amperage sensor	SEN0214, Gravity series, Dfrobot, Shanghai, China.	±20A DC	±1%
Voltage sensor	1135-Precision voltage sensor, Phidgets Inc., Calgary, Canada.	±30 V	±2%
Encoder	M-260, Encoder Products Co., Sagle, Idaho, USA.	4000(cycles/ revolution)	0.6 arc minutes
Load cell	TAS501, HT Sensor Technology Co., Ltd, Xi'an, China.	200 kg	±0.02%
Protractor	Mini-MAG, Fowler high precision, Newton, Massachusetts, USA	360° (4 x 90°)	±0.2°%
Cone penetrometer	CP40III, Rimik Pvt. Ltd., Toowoomba, Australia.	5600 kPa	-
Bulk density soil sampling kit	AMS Inc., American Falls, Idaho, USA.	-	-

the F_{DP} from zero to the maximum F_{DP} until the AGV is immobilized and the track starts slipping. Each experiment was replicated three times and proceeded as per Table 4. The experimental setup for conducting the DP test was shown in Fig. 1.

2.3. Data processing

For each combination of experiments, the collected sensor data were used to compute the response variables. The AGV's reference velocity (v_{ref}) is computed from track encoder data and track rolling radius. The AGV's actual velocity (v) was computed from the ground truth encoder data. The applied DP force (F_{DP}) was computed from the recorded load cell data and power consumption (P) with amperage and voltage sensor data. The travel reduction ratio (TRR) is a measure of the AGV's travel efficiency and is computed by Eq. 1.

$$TRR = 1 - \frac{v}{v_{ref}} \tag{1}$$

Tractive efficiency (TE) indicates how efficiently the AGV transfers the electrical power (P) to an available drawbar power and is defined by Eq. 2. The Power Number (PN) is defined as the power being used to normalize the AGV's weight (w) and velocity (v) (Eq. 3) and quantify the mobility energy costs (Eq. 3). The statistics of the computed response data are presented in Table 5.

$$TE = \frac{F_{DP} \times v}{P} \tag{2}$$

$$PN = \frac{P}{w \times v} \tag{3}$$

2.4. ANN model development

ANNs are adaptive systems using interconnected computational units called neurons arranged in a layered structure, and able to learn a complex and nonlinear relationship between inputs and outputs. ANNs integrate several distinct information processing layers (eg., input, hidden, and output layers) composed of nodes ("neurons") with weighted interconnections that present the previous layer's output to the next layer as inputs. Each node has an activation function, which converts its inputs to outputs. In the learning phase, the interconnection weights are iteratively adjusted according to a specified learning method until the desired output is obtained for each training sample.

The development of an ANN model with linearly dependent inputs is a methodological mistake (Pentos and Pieczarka, 2017). Linearly correlated inputs may lead to a multi-colinearity problem (Wu et al., 2014; Lee et al., 2020). Therefore, before developing an ANN model, possible linear correlations between inputs were examined by computing the Pearson correlation coefficients. A multi- layer perceptron (MLP) ANN trained with the Levenberg–Marquardt back-propagation (LMBP) algorithm was implemented as shown in Fig. 2. The inputs to the ANN were slope, speed and drawbar pull and a single response neuron produced the output. Therefore, three independent predictive ANN models were developed: ANN-TE, ANN-TRR and ANN-PN.

Table 4
Predicator and response variables used in the study.

Predicator			Response
Slope, degrees	Speed, m/min	Drawbar pull, N	
0	1	Variable pull, 0–1500 N	Tractive efficiency (TE)
10[d]	2		Travel reduction ratio (TRR)
18[d]	3		Power Number (PN)
-10[u]	4		
-18[u]	5		

[d] downhill slope
[u] uphill slope

Table 5
Statistics of experimental data for the response variable.

Response	Minimum	Maximum	Mean	Standard deviation
Tractive efficiency (TE)	0.00	0.48	0.14	0.09
Travel reduction ratio (TRR)	0.02	1.00	0.33	0.33
Power number (PN)	0.77	20*	6.07	5.59

* PN explodes to infinity (when TRR = 1), therefore upper limit 20 is considered.

The flowchart of ANN model development is shown in Fig. 3. The data pre-processing step includes the input data normalization to a mean zero and unit variance. The pre-processing facilitates network training process to extract the relevant information as well as to speed up the training. In MLP, the input and output layer neurons are decided by the number of model input and output variables, respectively. The number of neurons in the hidden layer significantly influences the model performance but there is no analytical solution available to determine how many to use. Thus, this choice is usually left to trial and error (Almaliki et al., 2016; Pentos and Pieczarka, 2017; Shafaei et al., 2018). In this study, the number of neurons in the hidden layer was varied from 3 to 30 for each ANN model, with each additional neuron increasing the ANN complexity. The neuron weights and biases are randomly initialized and then iteratively adjusted by the LMBP algorithm to minimize prediction errors against the set of training data (Hagan and Menhaj, 1994; Yu and Wilamowski, 2018). An early stopping criteria was used to prevent model overfitting – namely, training is stopped when the validation set performance increases for a set number of iterations (here 6). The weights and biases at the minimum of the validation error are preserved. Two different nonlinear activation functions (i.e., log-sigmoid and hyperbolic-tangent sigmoid) were evaluated for use in the hidden layer to capture the complex and non-linear relationships within data. A linear activation function (purelin) was used in the output layer because the target variables were continuous. The various numbers of hidden neurons (3–30) in combination with the two different activation functions generate 56 independent ANN structures for each output variable.

A re-sampling-based model validation technique called K-fold cross-validation (CV) was employed to elect the best ANN from each set of 56 ANN and to estimate the generalization error (Breiman and Spector, 1992; Setiono, 2001). In K-fold CV, the traction data (1288 observation) was divided into K (here 10), approximately equal-sized and non-overlapping subsets. The ANN was trained on eight subsets (1032 observations) and the remaining two subsets (each 128 obs.) served, respectively, as an early-stopping validation set to prevent over-fitting and a test set to assess model performance. This process was repeated ten times, selecting alternate subset to train each ANN structure and to asses performance on the corresponding test subset. The model performance was evaluated with two metrics: Mean Square Error (MSE) and Coefficient of determination (R^2). Each ANN model was trained on ten different non-overlapping data subsets, provided that each subset appeared in the test set once and the mean and variance of MSE and R^2 were computed over 10 runs (Fig. 3). For each dependent variable, the network with the lowest MSE and the highest R^2 on the test set was selected among the series of ANNs. This best performing ANN structure was finally trained on the entire dataset, and split randomly into training (90%), and validation (10%) sets. The weights and biases of the final predictive ANN models were saved in a computer for each dependent variable. During prediction, the ANN model provides a respective output in its original units.

2.5. Uncertainty analysis

The ANN model predictions are not certain and the prime source of

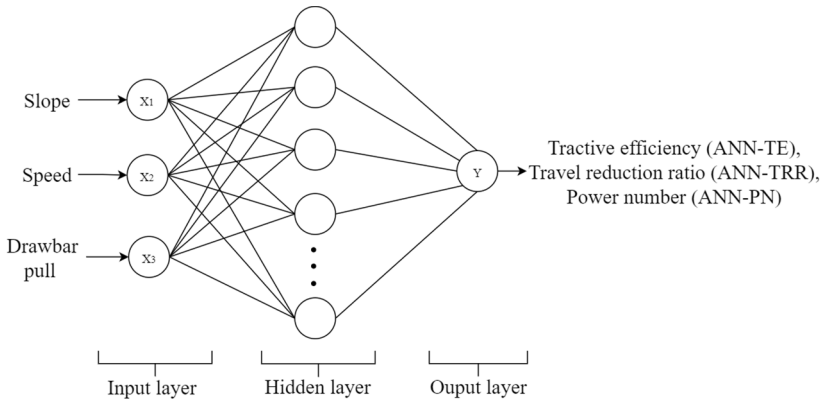

Fig. 2. Multi-layer percepron ANN architecture implemented in study.

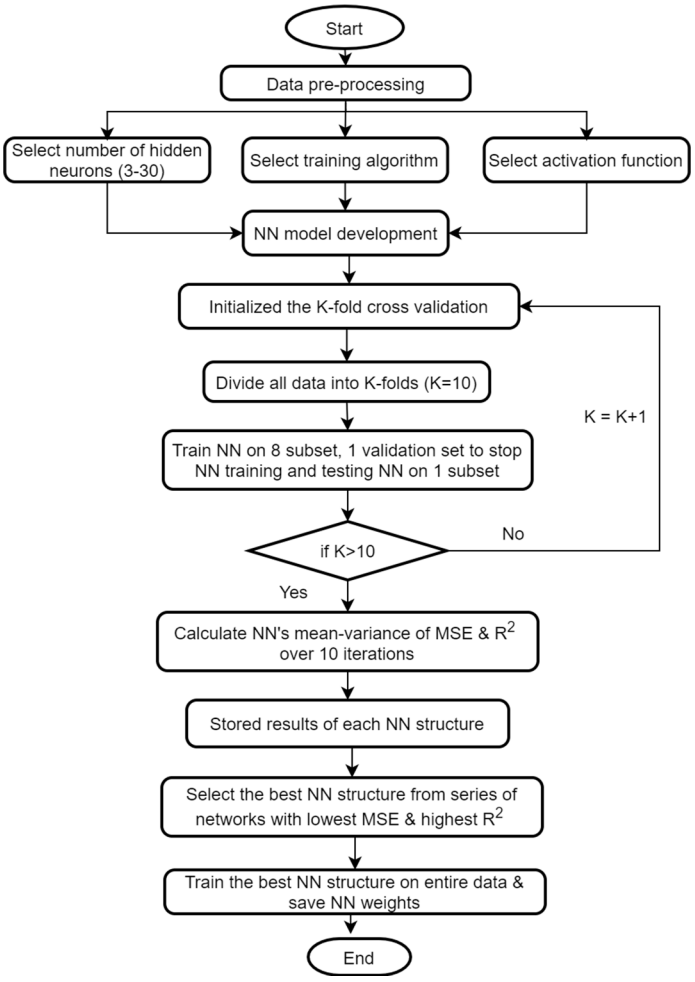

Fig. 3. Flowchart for selection of the best multi-layer feed forward network architecture.

this uncertainty emerges from random initialization of weights-biases, training data splitting methods, and selection of ANN structure (Talebizadeh et al., 2010; Tapoglou et al., 2018; Gao et al., 2018). In this study, the uncertainty analysis was performed on the final predictive models, keeping the ANN structure fixed, and the uncertainties emerging from random training data sampling and random weight initialization were quantified. This uncertainty analysis shows the effect of model inputs or model parameters on the ANN simulations results. A Monte Carlo simulation (MCS) was performed to quantify the uncertainty of the final predictive ANN model. MCS involves a retraining the ANN multiple times (here 1000) on randomly re-sampled data without replacement, maintaining the train-validation-test set ratio unchanged. Thus, a single ANN structure trained with MCS, generates 1000 outputs corresponding to each observed output. Therefore, a cumulative distribution function of the output was constructed. The 95 percent prediction uncertainties/interval (95 PPU) was determined from the associated output distribution by taking the 2.5th (X_L) and 97.5th (X_U) percentiles (Noori et al., 2010). The 95 PPU interval provides the range of prediction associated with the ANN model. The ANN uncertainty was expressed interms of the degree of uncertainty $\overline{d_x}$ and the percentage of

true data bracketed by the 95 PPU interval as suggested by (Abbaspour et al., 2007; Noori et al., 2010).

$$\overline{d_x} = \frac{1}{n}\sum_{i=1}^{n}\left(X_U - X_L\right)$$

where, n is the number of true observations. The ideal model delivers 100% of the observations bracketed by 95 PPU and $\overline{d_x}$ reaches to zero. However, the ideal results are not achievable, because of model uncertainty. Thus, a reasonable measure of $\overline{d_x}$ is calculated by d-factor as follows (Abbaspour et al., 2007; Noori et al., 2010):

$$d-factor = \frac{\overline{d_x}}{\sigma_x}$$

where, σ_x is the standard deviation of the output variable X. The larger d-factor, the higher the uncertainty and vice versa (Abbaspour et al., 2007); values less than 1 are desirable. The true data bracketed by 95 PPU are calculated as follows (Noori et al., 2010) and a higher percentage of 95 PPU is desirable:

$$Bracketed\ by\ 95\ PPU = \frac{1}{n}\ count\left(X|.X_L \leqslant X \leqslant X_U\right) \times 100$$

3. Results and Discussions

3.1. ANN models

Table 6 shows the Pearson Correlation coefficients between the ANN input variables. A very weak correlation was observed between the speed-slope and speed-drawbar pull, with a coefficient value of 0.01 and 0.06, respectively. A drawbar pull-slope exhibits a positive weak correlation with a coefficient value of 0.39. DP is found to be correlated with other two ANN inputs (speed and slope), with p-value less than 0.05. However, DP and speed are a major indicator of AGV's traction performance (TE, TRR and PN) and must be taken into account as input variables. Hence, all three predictors were included in ANN model development.

The performance of the ANN was observed on the test set and the performance statistics (MSE and R^2) of the five best ANN structures for ANN-TE, ANN-TRR and ANN-PN and are summarized in Table 7. Lower MSE and higher R^2 values are better. Boldfaced table entries indicate the optimal combinations of hidden layer sizes and activation functions for each output variable. The optimum numbers of hidden neurons were 22, 22 and 30 for ANN-TE, ANN-TRR and ANN-PN, respectively. Tansig was the best activation function for ANN-TE, ANN-TRR and logsig for ANN-PN. The final ANN model was trained on an entire data set and the results are presented in Table 8. A high value of R^2 (>0.90) and low value of MSE on the training, validation and entire data sets was obtained for ANN-TE showing the high model quality. The R^2 of ANN-TRR and ANN-PN models were ranged between 0.84–0.88% which is considered satisfactory model performance. A comparatively high sample standard deviation of ANN-TRR (0.33) and ANN-PN (5.6) (Table 5) explains the lower value of R^2.

The regression analysis and residual distribution of the ANN-TE, ANN-TRR and ANN-PN models are depicted in Figs. 4–6, respectively. A high regression correlation was observed for ANN-TE and ANN-TRR as shown in Figs. 4a and 5a, a R^2 of 0.933 and 0.88, respectively. The closeness of the scattered data to a unity slope indicates the good performance. Moreover, no definite pattern was observed in the model residuals for ANN-TE, ANN-TRR and ANN-PN as shown in Figs. 4b, 5b and 6b.

The developed traction models successfully demonstrate the ability of ANN to explain a non-linear, complex, and ill-defined relationship of small track ground vehicle traction behavior on sloping terrain as a function of slope, speed, and applied drawbar load. Once trained, ANN models predict the desired output with good generalization ability at a very high speed, indicating that ANN models are fast, accurate, and reliable. The results of this study are in good agreement with the previous similar studies conducted on the agricultural tillage and traction domain. These studies include ANN modeling on laboratory traction data obtained on radial tractor tires (Ekinci et al., 2015), ANN model development on data obtained from tractor-implement studies at different field conditions (Almaliki et al., 2016), and validation of ANN framework for predicting the tractive efficiency of four-wheel drive agricultural tractor (Shafaei et al., 2018). The studies mentioned above reported the R^2 higher than 90% for the developed ANN model, which shows ANN can capture the input and output relationship with better accuracy. The ANN-based model offers multiple benefits such as speed, robustness, and accuracy than the traditional modeling approach, including analytical, empirical, and semi-empirical methods. The ANN-based approach would be the best alternative to model intricate agricultural soil, tillage, and traction interactions.

Fig. 7 shows the effectiveness of an early stopping method to prevent overfitting on ANN-TE. It stops the training at a point when validation performance starts to degrade (Fig. 7b). Without the early stopping method, the validation set is absent, and the ANN will train for a set number of epochs. This overfits the training data and poor performance is observed on the test set (Fig. 7a).

3.2. Uncertainty analysis

The MCS uncertainty analysis was conducted on the final ANN structure for each output variable and the results are summarized in Table 9. A 95 PPU for each output variable is shown in Fig. 8. The 95 PPU exhibits reasonable general behavior for the true observations, although a few observations tend to exceed the lower and upper bound, as shown in Fig. 8.

The wider the 95 PPU, the lower the ANN prediction accuracy and vice versa (Noori et al., 2010). Fig. 8 depicts a wider prediction interval for ANN-PN and ANN-TRR compared to ANN-TE, hence, a greater d-factor was reported for ANN-PN (0.42) and ANN-TRR (0.41) compared to ANN-TE (0.28) which explains the degree of uncertainty associated with each model. Therefore, the ANN-PN and ANN-TRR exhibit higher uncertainty compared to ANN-TE. However, the wider prediction interval encloses a relatively higher number of predictions bracketed by 95 PPU for ANN-PN (79%) and ANN-TRR (64%) compared to ANN-TE (60%) as shown in Table 9. The 95 PPU explains the robustness of the final ANN model. The average distance between the lower and upper bounds of predictive interval is explained by the $\overline{d_x}$. The d-factor lower than 1 is acceptable, thus, all three ANN models are within an acceptable limit. MCS uncertainty analysis explains the robustness and reliability of the developed ANN models. The constructed prediction interval can be used for decision making of AGV operation on sloped terrain and computer simulations.

Table 6
Pearson's coefficient (lower left to diagonal) and p-values (α =5%) (upper right to diagonal) for predictor variables.

	Slope	Speed	Drawbar pull
Slope	1	0.60	0.00
Speed	0.01	1	0.02
Drawbar pull	0.39	0.06	1

4. Conclusions

In this study, we investigated the ability of ANN to predict the traction performance of the AGV on slopes in terms of TE, TRR and PN as a function of the AGV's speed, applied drawbar pull and testbed slope. A series of ANN of increasing in complexity were developed for each output variable and the 10-fold CV was used to check the generalization

Table 7
K-fold cross-validation results for five best models on the test set.

Predictor	ANN	Hidden-layer activation	MSE_{mean}	MSE_{min}	MSE_{std}	R^2_{mean}	R^2_{max}	R^2_{std}
TE	3–20-1	Logsig	0.0007	0.0004	0.0002	0.917	0.942	0.017
	3–22-1	**Tansig**	**0.0007**	**0.0004**	**0.0002**	**0.919**	**0.938**	**0.018**
	3–25-1	Logsig	0.0007	0.0004	0.0002	0.917	0.940	0.017
	3–26-1	Tansig	0.0007	0.0004	0.0002	0.915	0.937	0.021
	3–29-1	Logsig	0.0007	0.0004	0.0002	0.917	0.937	0.019
TRR	**3–22-1**	**Tansig**	**0.016**	**0.011**	**0.004**	**0.847**	**0.900**	**0.038**
	3–25-1	Logsig	0.016	0.010	0.004	0.844	0.904	0.042
	3–26-1	Tansig	0.016	0.012	0.003	0.846	0.894	0.037
	3–27-1	Tansig	0.016	0.011	0.003	0.843	0.896	0.040
	3–29-1	Tansig	0.016	0.011	0.004	0.844	0.900	0.043
PN	3–23-1	Logsig	5.65	3.31	1.76	0.821	0.883	0.058
	3–26-1	Tansig	5.55	3.37	1.41	0.821	0.883	0.050
	3–27-1	Tansig	5.58	3.58	1.39	0.823	0.872	0.043
	3–30-1	**Logsig**	**5.51**	**3.63**	**1.20**	**0.826**	**0.872**	**0.039**
	3–30-1	Tansig	5.57	3.63	1.40	0.823	0.876	0.046

Table 8
Parameters of ANN's used as a best neural models.

Predictor	ANN structure	MSE			R^2		
		train data set	validation data set	all data set	train data set	validation data set	all data set
TE	3–22-1	0.0005	0.0008	0.0006	0.936	0.902	0.933
TRR	3–22-1	0.012	0.015	0.012	0.886	0.847	0.882
PN	3–30-1	4.45	4.42	4.44	0.859	0.841	0.858

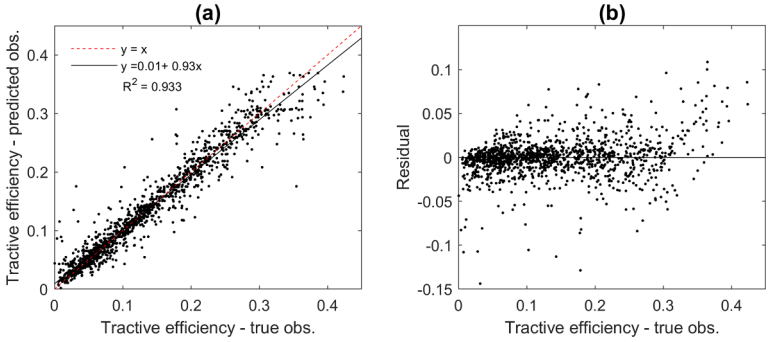

Fig. 4. ANN-TE (a) regression between predicted against true obs. (b) distribution of model residuals.

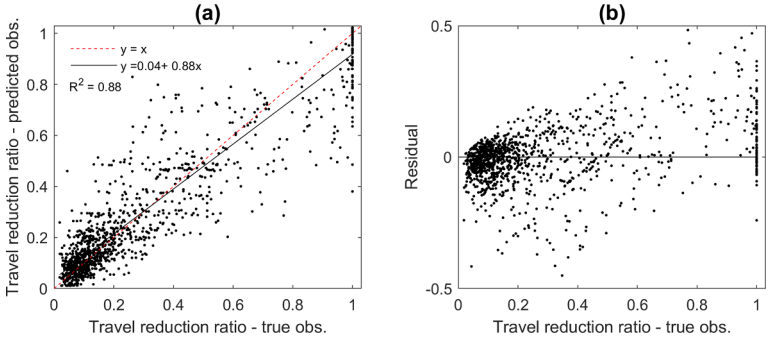

Fig. 5. ANN-TRR (a) regression between predicted against true obs. (b) distribution of model residuals.

ability on the test set. For each output variable, the best ANN structure was identified and a final predictive model trained on the entire data set. A Monte-Carlo simulation analysis (1000 runs) was performed separately on the selected ANN structures. The following conclusions can be drawn from this study,

- A three-layer ANN architecture with a nonlinear activation function predicts the traction performance of AGV with a good generalization ability.
- ANN structure influences the model performance and increasing the size of the hidden layer ensures improved performance before the start of data overfitting. The optimum number of hidden neurons for TE, TRR and PN were 22, 22 and 30, respectively.

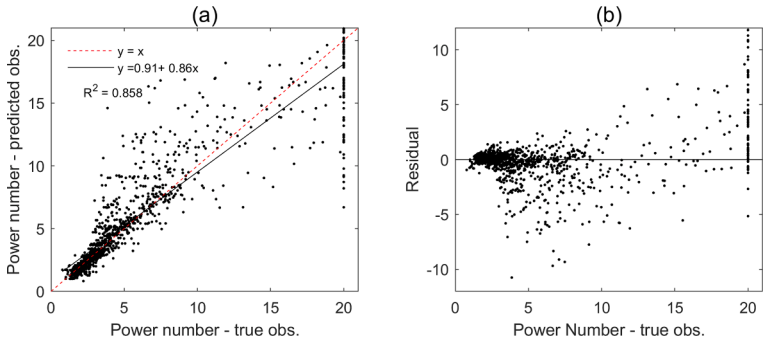

Fig. 6. ANN-PN (a) regression between predicted against true obs. (b) distribution of model residuals.

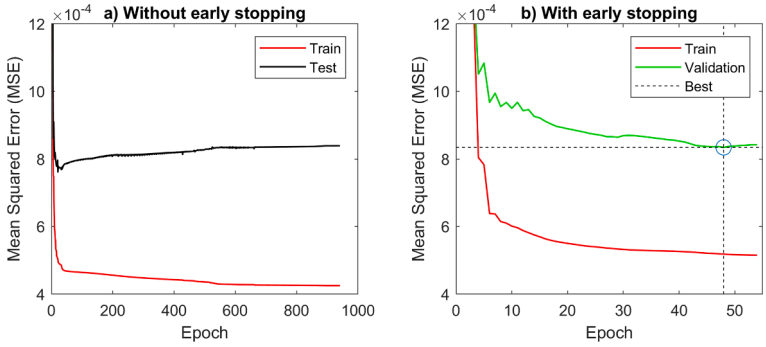

Fig. 7. Early stopping criteria: Overfitting prevention strategy for ANN-TE.

Table 9
Results of uncertainty analysis of ANN models.

Dependent variable	ANN structure	$\overline{d_x}$	d-factor	Bracketed by 95 PPU (%)
TE	3-22-1	0.03	0.28	60
TRR	3–22-1	0.13	0.41	64
PN	3–30-1	2.38	0.42	79

- MCS based uncertainty analysis further strengthens the ANN ability to predict the AGV's traction performance by constructing 95% prediction intervals. It quantifies the reliability and robustness of ANN model output. The degree of uncertainty was in acceptable limits for all models, even-though, a few observed data points were outside the 95% prediction interval.
- ANNs are fast, accurate, and reliable tools to predict AGV traction performance in a sloped soil bin.

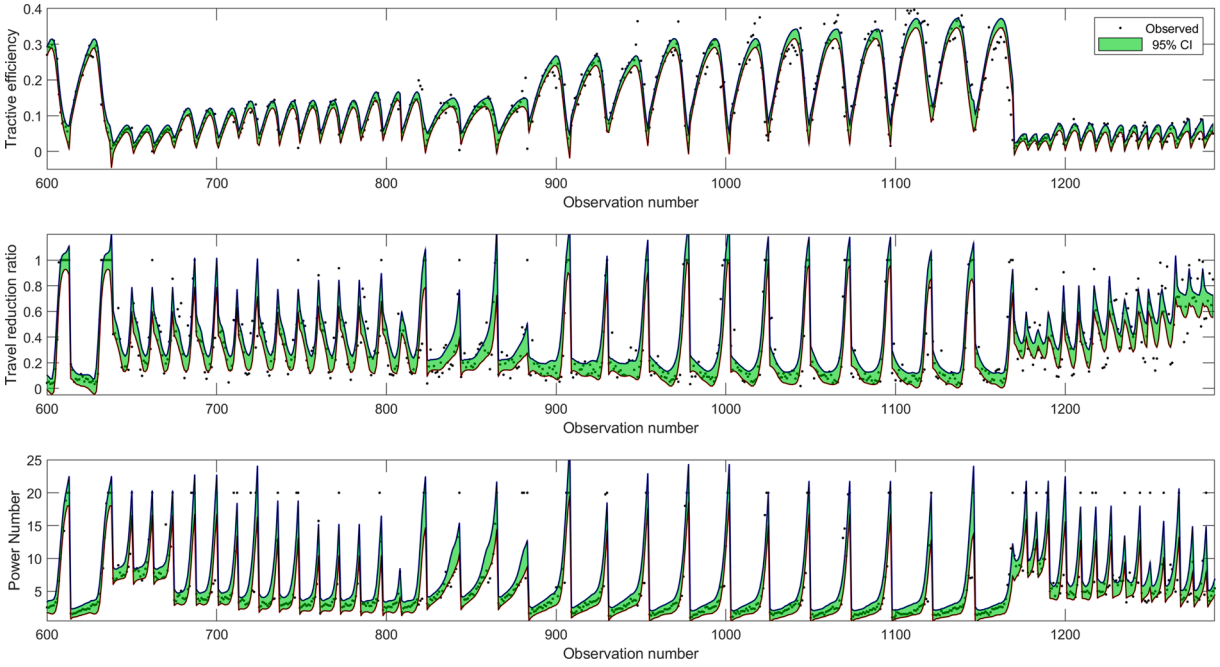

Fig. 8. 95% PPU for (a) TE-ANN, (b) ANN-TRR and (c) ANN-PN.

- Such predictive traction models can empower the entire multi-AGV system operation in a dynamic agricultural environment by assisting in vehicle control variables optimization, establishing the vehicle boundary conditions on slopes, energy optimization and decision making regarding the application feasibility, and go-no-go situation ahead of time.

Funding

This study was financially supported by a National Institute of Food and Agriculture (NIFA–USDA). The project is titled "National Robotics Initiative (NRI): Multi-Robot Farming on Marginal, Highly Sloped Lands" Project number- KS4513081.

CRediT

Chetan Badgujar: Conceptualization, Methodology, Data collection, Data curation, Software. Daniel Flippo.: Visualization, Investigation, Supervision, Writing- Original draft preparation. Stephen Welch.: Data curation, model building and Validation, Supervision, Reviewing and Editing.

Declaration of Competing Interest

The authors declare that they have no known competing financial interests or personal relationships that could have appeared to influence the work reported in this paper.

References

Abbaspour, K.C., Yang, J., Maximov, I., Siber, R., Bogner, K., Mieleitner, J., et al., 2007. Modelling hydrology and water quality in the pre-alpine/alpine Thur watershed using SWAT. J. Hydrol. 333 (2–4), 413–430. https://doi.org/10.1016/j.jhydrol.2006.09.014.

Almaliki, S., Alimardani, R., Omid, M., 2016. Artificial Neural Network Based Modeling of Tractor Performance at Different Field Conditions. Agric. Eng. Int.: CIGR J. 18 (4), 262–274.

Amrita, S.A., Abirami, E., Ankita, A., Praveena, R., Srimeena, R., 2015. Agricultural Robot for automatic ploughing and seeding. In: 2015 IEEE Technological Innovation in ICT for Agriculture and Rural Development (TIAR). doi:10.1109/TIAR.2015.7358525.

Antanasijevic, D., Pocajt, V., Peric-Grujic, A., Ristic, M., 2014. Modelling of dissolved oxygen in the Danube River using artificial neural networks and Monte Carlo Simulation uncertainty analysis. J. Hydrol. 519, 1895–1907. https://doi.org/10.1016/j.jhydrol.2014.10.009.

Bayar, G., Bergerman, M., Koku, A.B., Konukseven, E.i., 2015. Localization and control of an autonomous orchard vehicle. Comput. Electron. Agric. 115, 118–128. https://doi.org/10.1016/j.compag.2015.05.015.

Bechar, A., Vigneault, C., 2016. Agricultural robots for field operations: Concepts and components. Biosyst. Eng. 149, 94–111. https://doi.org/10.1016/j.biosystemseng.2016.06.014.

Breiman, L., Spector, P., 1992. Submodel selection and evaluation in regression. The x-random case. International Statistical Review 60 (3), 291. https://doi.org/10.2307/1403680.

Burt, E.C., Reaves, C.A., Bailey, A.C., Pickering, W.D., 1980. A Machine for Testing Tractor Tires in Soil Bins. Transactions of the ASAE 23 (3), 0546–0547. https://doi.org/10.13031/2013.34620.

Choi, K.H., Han, S.K., Han, S.H., Park, K.H., Kim, K.S., Kim, S., 2015. Morphology-based guidance line extraction for an autonomous weeding robot in paddy fields. Comput. Electron. Agric. 113, 266–274. https://doi.org/10.1016/j.compag.2015.02.014.

Colin, A., Burt, E.C., Turner, J.L., 1987. An Empirical Equation for Predicting Tractive Performance of Log-Skidder Tires. Transactions of the ASAE 30 (5), 1231–1236. https://doi.org/10.13031/2013.30550.

Conesa-Muñoz, J., Gonzalez-de Soto, M., Gonzalez-de Santos, P., Ribeiro, A., 2015. Distributed Multi-Level Supervision to Effectively Monitor the Operations of a Fleet of Autonomous Vehicles in Agricultural Tasks. Sensors 15 (3), 5402–5428. https://doi.org/10.3390/s150305402.

Creager, C., Asnani, V., Oravec, H., Woodward, A., 2017. Drawbar Pull (DP) Procedures for Off-Road Vehicle Testing. Tech. Rep. NASA/TP-2017-219384, E-19292, GRC-E-DAA-TN31725.

De-An, Z., Jidong, L., Wei, J., Ying, Z., Yu, C., 2011. Design and control of an apple harvesting robot. Biosyst. Eng. 110 (2), 112–122. https://doi.org/10.1016/j.biosystemseng.2011.07.005.

Dehghani, M., Saghafian, B., Saleh, F.N., Farokhnia, A., Noori, R., 2014. Uncertainty analysis of streamflow drought forecast using artificial neural networks and Monte-Carlo simulation. Int. J. Climatol. 34 (4), 1169–1180. https://doi.org/10.1002/joc.3754.

Domier, K., Willans, A., 1978. Tractive efficiency–maximum or optimum? Transactions of the ASAE 21 (4), 650–0653.

Dwyer, M., 1987. Prediction of drawbar test performance. J. Terrramech. 24 (2), 169–177. https://doi.org/10.1016/0022-4898(87)90007-3.

Ekinci, S., Carman, K., Kahramanli, H., 2015. Investigation and modeling of the tractive performance of radial tires using off-road vehicles. Energy 93, 1953–1963. https://doi.org/10.1016/j.energy.2015.10.070.

Emmi, L., Paredes-Madrid, L., Ribeiro, A., Pajares, G., Gonzalez-de-Santos, P., 2013. Fleets of robots for precision agriculture: a simulation environment. Industrial Robot: An International Journal 40 (1), 41–58. https://doi.org/10.1108/01439911311294246.

Emmi, L., Gonzalez-de Soto, M., Pajares, G., Gonzalez-de Santos, P., 2014. New Trends in Robotics for Agriculture: Integration and Assessment of a Real Fleet of Robots. The Scientific World Journal 2014, 1–21. https://doi.org/10.1155/2014/404059.

Foley, J.A., Ramankutty, N., Brauman, K.A., Cassidy, E.S., Gerber, J.S., Johnston, M., et al., 2011. Solutions for a cultivated planet. Nature 478 (7369), 337–342. https://doi.org/10.1038/nature10452.

Freitag, D., 1966. A dimensional analysis of the performance of pneumatic tires on clay. J. Terrramech. 3 (3), 51–68. https://doi.org/10.1016/0022-4898(66)90106-6.

Gao, M., Yin, L., Ning, J., 2018. Artificial neural network model for ozone concentration estimation and Monte Carlo analysis. Atmos. Environ. 184, 129–139. https://doi.org/10.1016/j.atmosenv.2018.03.027.

García-Pérez, L., García-Alegre, M.C., Ribeiro, A., Guinea, D., 2008. An agent of behaviour architecture for unmanned control of a farming vehicle. Comput. Electron. Agric. 60 (1), 39–48. https://doi.org/10.1016/j.compag.2007.06.004.

Gonzalez-De-Santos, P., Fernández, R., Sepúlveda, D., Navas, E., Armada, M., 2020. Unmanned Ground Vehicles for Smart Farms. In: Intechopen, Agronomy. Climate Change and Food Security. https://doi.org/10.5772/intechopen.90683.

Gregory, P.J., George, T.S., 2011. Feeding nine billion: the challenge to sustainable crop production. J. Exp. Bot. 62 (15), 5233–5239. https://doi.org/10.1093/jxb/err232.

Hagan, M., Menhaj, M., 1994. Training feedforward networks with the Marquardt algorithm. IEEE Trans. Neural Networks 5 (6), 989–993. https://doi.org/10.1109/72.329697.

Haibo, L., Shuliang, D., Zunmin, L., Chuijie, Y., 2015. Study and Experiment on a Wheat Precision Seeding Robot. Journal of Robotics 2015, 1–9. https://doi.org/10.1155/2015/696301.

Hayes, J., Ligon, J., 1981. Traction Prediction Using Soil Physical Properties. Transactions of the ASAE 24 (6), 1420–1425. https://doi.org/10.13031/2013.34464.

Huang, Y., Lan, Y., Thomson, S.J., Fang, A., Hoffmann, W.C., Lacey, R.E., 2010. Development of soft computing and applications in agricultural and biological engineering. Comput. Electron. Agric. 71 (2), 107–127. https://doi.org/10.1016/j.compag.2010.01.001.

Hu, J., Yan, X., Ma, J., Qi, C., Francis, K., Mao, H., 2014. Dimensional synthesis and kinematics simulation of a high-speed plug seedling transplanting robot. Comput. Electron. Agric. 107, 64–72. https://doi.org/10.1016/j.compag.2014.06.004.

IS 2720–2, 1993. Methods of test for soils, part 2: Determination of water content [CED 43: soil and foundation engineering]. Bureau of Indian Standards.

Jagbrant, G., Underwood, J.P., Nieto, J., Sukkarieh, S., 2015. LiDAR Based Tree and Platform Localisation in Almond Orchards. Springer International Publishing. p. 469–483, ISBN 978-3-319-07488-7; 2015. doi:10.1007/978-3-319-07488-7_32.

Lee, J., Kim, C.G., Lee, J.E., Kim, N.W., Kim, H., 2020. Medium-Term Rainfall Forecasts Using Artificial Neural Networks with Monte-Carlo Cross-Validation and Aggregation for the Han River Basin, Korea. Water 12 (6), 1743.

Li, Z., Li, P., Yang, H., Wang, Y., 2013. Stability tests of two-finger tomato grasping for harvesting robots. Biosyst. Eng. 116 (2), 163–170. https://doi.org/10.1016/j.biosystemseng.2013.07.017.

Li, N., Remeikas, C., Xu, Y., Jayasuriya, S., Ehsani, R., 2015. Task Assignment and Trajectory Planning Algorithm for a Class of Cooperative Agricultural Robots. J. Dyn. Syst. Meas. Contr. 137 (051004) https://doi.org/10.1115/1.4028849.

Marcé, R., Comerma, M., García, J.C., Armengol, J., 2004. A neuro-fuzzy modeling tool to estimate fluvial nutrient loads in watersheds under time-varying human impact. Limnology and Oceanography: Methods 2 (11), 342–355. https://doi.org/10.4319/lom.2004.2.342.

Mehta, S., Burks, T., 2014. Vision-based control of robotic manipulator for citrus harvesting. Comput. Electron. Agric. 102, 146–158. https://doi.org/10.1016/j.compag.2014.01.003.

Myers, J.R., Hendricks, K.J., 2010. Agricultural tractor overturn deaths: Assessment of trends and risk factors. Am. J. Ind. Med. 53 (7), 662–672. https://doi.org/10.1002/ajim.20775.

Myers, M.L., Cole, H.P., Westneat, S.C., 2009. Injury severity related to overturn characteristics of tractors. Journal of Safety Research 40 (2), 165–170. https://doi.org/10.1016/j.jsr.2009.02.007.

Nakashima, H., Oida, A., 2004. Algorithm and implementation of soil-tire contact analysis code based on dynamic FE–DE method. J. Terrramech. 41 (2–3), 127–137. https://doi.org/10.1016/j.jterra.2004.02.002.

Noori, R., Hoshyaripour, G., Ashrafi, K., Araabi, B.N., 2010. Uncertainty analysis of developed ANN and ANFIS models in prediction of carbon monoxide daily concentration. Atmos. Environ. 44 (4), 476–482. https://doi.org/10.1016/j.atmosenv.2009.11.005.

Pentos, K., Pieczarka, K., 2017. Applying an artificial neural network approach to the analysis of tractive properties in changing soil conditions. Soil and Tillage Research 165, 113–120. https://doi.org/10.1016/j.still.2016.08.005.

Pentos, K., Pieczarka, K., Lejman, K., 2020. Application of Soft Computing Techniques for the Analysis of Tractive Properties of a Low-Power Agricultural Tractor under

Various Soil Conditions. Complexity 2020, 1–11. https://doi.org/10.1155/2020/7607545.
Pérez-Ruíz, M., Slaughter, D.C., Fathallah, F.A., Gliever, C.J., Miller, B.J., 2014. Co-robotic intra-row weed control system. Biosyst. Eng. 126, 45–55. https://doi.org/10.1016/j.biosystemseng.2014.07.009.
Se, S., Lowe, D., Little, J., 2005. Vision-based global localization and mapping for mobile robots. IEEE Trans. Rob. 21 (3), 364–375. https://doi.org/10.1109/TRO.2004.839228.
Setiono, R., 2001. Feedforward neural network construction using cross validation. Neural Comput. 13 (12), 2865–2877. https://doi.org/10.1162/089976601317098565.
Shafaei, S., Loghavi, M., Kamgar, S., 2018. An extensive validation of computer simulation frameworks for neural prognostication of tractor tractive efficiency. Comput. Electron. Agric. 155, 283–297. https://doi.org/10.1016/j.compag.2018.10.027.
Standards, ASAE, 2019. Procedures for Using and Reporting Data Obtained with the Soil Cone Penetrometer, EP542.. ASABE Technical Information Library.
Sunusi, I.I., Zhou, J., Zhen Wang, Z., Sun, C., Eltayeb Ibrahim, I., Opiyo, S., et al., 2020. Intelligent tractors: Review of online traction control process. Comput. Electron. Agric. 170, 105176. https://doi.org/10.1016/j.compag.2019.105176.
Taghavifar, H., Mardani, A., 2014. Application of artificial neural networks for the prediction of traction performance parameters. Journal of the Saudi Society of Agricultural Sciences 13 (1), 35–43. https://doi.org/10.1016/j.jssas.2013.01.002.
Taghavifar, H., Mardani, A., 2014. Use of artificial neural networks for estimation of agricultural wheel traction force in soil bin. Neural Comput. Appl. 24 (6), 1249–1258. https://doi.org/10.1007/s00521-013-1360-8.
Taghavifar, H., Mardani, A., Hosseinloo, A.H., 2015. Appraisal of artificial neural network-genetic algorithm based model for prediction of the power provided by the agricultural tractors. Energy 93, 1704–1710. https://doi.org/10.1016/j.energy.2015.10.066.
Talebizadeh, M., Morid, S., Ayyoubzadeh, S.A., Ghasemzadeh, M., 2010. Uncertainty Analysis in Sediment Load Modeling Using ANN and SWAT Model. Water Resour. Manage 24 (9), 1747–1761. https://doi.org/10.1007/s11269-009-9522-2.
Tapoglou, E., Varouchakis, E.A., Karatzas, G.P., 2018. Uncertainty estimations in different components of a hybrid ANN - fuzzy - kriging model for water table level simulation. In: 13th International Conference on Hydroinformatics (HIC 2018); vol. 3 of EPiC Series in Engineering. EasyChair; 2018, p. 2042–2050.
Tiwari, V., Pandey, K., Pranav, P., 2010. A review on traction prediction equations. J. Terrramech. 47 (3), 191–199. https://doi.org/10.1016/j.jterra.2009.10.002.
Tohmaz, A., Hassan, A., 1995. Application of artificial neural networks to skidder traction performance. J. Terrramech. 32 (3), 105–114. https://doi.org/10.1016/0022-4898(95)00010-0.
Upadhyaya, S., Wulfsohn, D., Jubbal, G., 1989. Traction prediction equations for radial ply tyres. J. Terrramech. 26 (2), 149–175. https://doi.org/10.1016/0022-4898(89)90004-9.
Wang, Z., Domier, K.W., 1989. Prediction of Drawbar Performance for a Tractor With Dual Tires. Transactions of the ASAE 32 (5), 1529–1533. https://doi.org/10.13031/2013.31184.
Wismer, R.D., Luth, H.J., 1974. Off-Road Traction Prediction for Wheeled Vehicles. Transactions of the ASAE 17 (1), 0008–0010. https://doi.org/10.13031/2013.36772.
Wong, J., 1986. Computer aided analysis of the effects of design parameters on the performance of tracked vehicles. J. Terrramech. 23 (2), 95–124. https://doi.org/10.1016/0022-4898(86)90017-0.
Wong, J.Y., 2010a. *Terramechanics and off-road vehicle engineering terrain behaviour, off-road vehicle performance and design* (2nd ed.). Oxford: Butterworth-Heinemann.
Wong, J., 2010b. Performance of off-road vehicles. In: Terramechanics and Off-Road Vehicle Engineering (Second Edition). Butterworth-Heinemann. ISBN 978-0-7506-8561-0, p. 129 – 153. doi: 10.1016/B978-0-7506-8561-0.00006-3.
Woodward, A.C., 2011. Experimental Analysis of the Effects of the Variation of Drawbar Pull Test Parameters for Exploration Vehicles on GRC-1 Lunar Soil Simulant. Thesis; Virginia Tech.
Wu, W., Dandy, G.C., Maier, H.R., 2014. Protocol for developing ANN models and its application to the assessment of the quality of the ANN model development process in drinking water quality modelling. Environmental Modelling & Software 54, 108–127. https://doi.org/10.1016/j.envsoft.2013.12.016.
Yong, R., Fattah, E., 1976. Prediction of wheel-soil interaction and performance using the finite element method. J. Terrramech. 13 (4), 227–240. https://doi.org/10.1016/0022-4898(76)90044-6.
Yu, H., Wilamowski, B.M., 2018. Levenberg-marquardt training. In: Intelligent Systems; 2 ed. CRC Press. p. 12–1, 2018–12–16. doi:10.1201/9781315218427-12.
Zabel, F., Delzeit, R., Schneider, J.M., Seppelt, R., Mauser, W., Václavík, T., 2019. Global impacts of future cropland expansion and intensification on agricultural markets and biodiversity. Nature Communications 10 (1), 2844. https://doi.org/10.1038/s41467-019-10775-z.
Zhang, C., Noguchi, N., Yang, L., 2016. Leader-follower system using two robot tractors to improve work efficiency. Comput. Electron. Agric. 121, 269–281. https://doi.org/10.1016/j.compag.2015.12.015.
Zhu, Z., Torisu, R., Takeda, J., Mao, E., Zhang, Q., 2005. Neural Network for estimating Vehicle Behaviour on Sloping Terrain. Biosyst. Eng. 91 (4), 403–411. https://doi.org/10.1016/j.biosystemseng.2005.05.003.